
Subgraph Matching via Query-Conditioned Subgraph Matching Neural Networks and Bi-Level Tree Search

Derek Xu*

University of California Los Angeles
derekxu@g.ucla.edu

Yunsheng Bai*

University of California Los Angeles
yba@g.ucla.edu

Yizhou Sun

University of California Los Angeles
yzsun@cs.ucla.edu

Wei Wang

University of California Los Angeles
weiwang@cs.ucla.edu

Abstract

Recent advances have shown the success of using reinforcement learning and search to solve NP-hard graph-related tasks, such as Traveling Salesman Optimization, Graph Edit Distance computation, etc. However, it remains unclear how one can efficiently and accurately detect the occurrences of a small query graph in a large target graph, which is a core operation in graph database search, biomedical analysis, social group finding, etc. This task is called Subgraph Matching which essentially performs subgraph isomorphism check between a query graph and a large target graph. One promising approach to this classical problem is the “learning-to-search” paradigm, where a reinforcement learning (RL) agent is designed with a learned policy to guide a search algorithm to quickly find the solution without any solved instances for supervision. However, for the specific task of Subgraph Matching, though the query graph is usually small given by the user as input, the target graph is often orders-of-magnitude larger. It poses challenges to the neural network design and can lead to solution and reward sparsity. In this paper, we propose N-BLS with two innovations to tackle the challenges: (1) A novel encoder-decoder neural network architecture to dynamically compute the matching information between the query and the target graphs at each search state; (2) A Monte Carlo Tree Search enhanced bi-level search framework for training the policy and value networks. Experiments on five large real-world target graphs show that N-BLS can significantly improve the subgraph matching performance.

1 Introduction

With the growing amount of graph data that naturally arises in many domains, solving graph-related tasks via machine learning has gained increasing attention. Many NP hard tasks, e.g. Traveling Salesman Optimization [46], Graph Edit Distance computation [44], Maximum Common Subgraph detection [2], have recently been tackled via learning-based methods. These works on the one hand rely on search to enumerate the large solution space, and on the other hand use reinforcement learning (RL) to learn a good search policy from training data, thus obviating the need for hand-crafted heuristics adopted by traditional solvers. Such learning-to-search paradigm [2] also allows the training the RL agent without any solved instances for supervision. However, how to design a neural network architecture under the RL-guided search framework remains unclear for the task

*Equal contribution.

of Subgraph Matching, which requires the detection of all occurrences of a small query graph in an orders-of-magnitude larger target graph. Subgraph Matching has wide applications in graph database search [23], knowledge graph query [16], biomedical analysis [49], social group finding [27], quantum circuit design [13], etc. As a concrete example, Subgraph Matching is used for protein complex search in a protein-protein interaction network to test whether the interactions within a protein complex in a species are also present in other species [4].

Due to its NP-hard nature, the state-of-the-art Subgraph Matching algorithms rely on backtracking search with various techniques proposed to reduce the large search space [38, 15, 43]. However, these techniques are mostly driven by heuristics, and as a result, we observe that such solvers often fail to find any solution on large target graphs under a reasonable time limit, although they tend to work well on small graph pairs. We denote this phenomenon as *solution sparsity*. Such solution sparsity requires the designed model to not only have enough capacity but also to run efficiently under limited computational budget. Another consequence of solution sparsity is that, there can be little-to-no reward signals for the RL agent under a self-play training framework [36], which we denote as *reward sparsity*.

In this paper, we propose N-BLS (*Neural Bi-level Search*) with two means to address the aforementioned challenges. First, we propose a novel graph encoder-decoder neural network to dynamically match the query graph with the target graph and perform aggregation operation only on the query graph to reduce information loss. The novel encoder decouples the intra-graph message passing module (the “propagation” module) that yields state-independent node embeddings, and the inter-graph message passing module (the “matching” module) that refines the node embeddings via subgraph-to-graph matching. Thus, the intra-graph embeddings can be computed only once at the beginning of search for efficient inference. We further advance the inter-graph message passing by propagating only between nodes that either are already matched or can be matched in future by running a local candidate search space computation algorithm at each search state. Such algorithm leverages the key requirement of Subgraph Matching that every node and edge in the query graph must be matched to the target graph, and therefore reduces the amount of candidates from all the nodes in the target graph to a much smaller amount. Compared with a Graph Matching Network [24] which computes all the pairwise node-to-node message passing between two input graphs, our matching module is able to focus on only the node pairs that can contribute to the solution, and thus is both more effective and more efficient. Second, to address the reward sparsity issue incurred by the size of the target graph, we augment the backbone backtracking search algorithm with an inner Monte Carlo Tree Search (MCTS) to refine the raw policy predicted by the neural network, yielding an improved search policy. This results in a bi-level search algorithm, where the outer backtracking search and the inner MCTS work together for the policy and value training. Experiments on real graph datasets demonstrate that N-BLS outperforms baseline solvers in terms of effectiveness by a large margin. Our contributions can be summarized as follows:

- We address the challenging yet important task of Subgraph Matching with a vast amount of practical applications and propose N-BLS as the solution.
- One key novelty is a proposed encoder layer consisting of a propagation module and a matching module that dynamically passes the information between the input graphs.
- The adoption of MCTS results in a bi-level search framework for effective training the policy and value networks, which is another novelty.
- We conduct extensive experiments on real-world graphs to demonstrate the effectiveness of the proposed approach compared against a series of strong baselines in Subgraph Matching.

2 Preliminaries

2.1 Problem Definition

We denote a query graph as $q = (V_q, E_q)$ and a target graph as $G = (V_G, E_G)$ where V and E denote the node and edge sets. q and G are associated with a node labeling function L_q which maps every node into a label l in a label set Σ . **Subgraph** For a subset of nodes S of V_q , $q[S]$ denotes the subgraph of q with an node set S and an edge set consisting of all the edges in E_q that have both endpoints in S . **Subgraph isomorphism** q is subgraph isomorphic to G if there exists an injective node-to-node mapping $M : V_q \rightarrow V_G$ such that (1) $\forall u \in V_q, L_q(u) = L_G(M(u))$; and (2)

$\forall e_{(u,u')} \in E_q, e_{(M(u),M(u'))} \in E_G$. **Subgraph Matching** The task of Subgraph Matching aims to find the subgraphs in G that are isomorphic to q . We call M a solution, or a match of q to G . We call a pair (q, G) is solved if the algorithm can find any match under a given time limit, which we find a challenge for existing solvers on input graphs in experiments.

2.2 Related Work

Non-learning methods on Subgraph Matching Existing methods on Subgraph Matching can be broadly categorized into backtracking search algorithms [34, 12, 11, 10, 15, 43] and multi-way join approaches [20, 21, 22, 14]. The former category of approaches employ a branch and bound approach to grow the solution from an empty subgraph by gradually seeking one matching node pair at a time following a strategic order until the entire search space is explored. The multi-way join approaches rely on decomposing the query graph into nodes and edges and performing join operations repeatedly to combine the partially matched subgraphs to q . However, they tend to work well on small query graphs generally with less than 10 nodes [38], and thus we follow and compare against methods in the former category, whose details will be shown in Section 2.3.

Learning-based methods for subgraph-related problems The idea of designing neural networks for predicting subgraph-graph relation has been explored, which due to its approximate nature may contain false positives/negatives, and it remains unclear how one can directly use these methods for exact Subgraph Matching. For example, NMATCH [26] learns node embeddings to predict a score for an input subgraph-graph pair indicating whether the subgraph is contained in another graph, which can be regarded as solving the approximate version of Subgraph Matching. Another direction of research aims to perform subgraph counting [25, 8] supervised on the number of specific substructures, and again lacks an explicitly search strategy and thus falls short of yielding solutions for Subgraph Matching.

Efforts on using RL for graph NP-hard problems The idea of using RL to replace heuristics in search algorithms for NP-hard graph-related tasks is not new, and we identify three works similar to the present work. (1) GLSEARCH [2] detects the maximum common subgraph (MCS) in an input graph pair, which is different from Subgraph Matching which requires the entire q to be matched with G , allowing further improvement in the neural network and search design. (2) RL-QVO [43] tackles Subgraph Matching via ordering the nodes in the *query* graph as a global pre-processing step before search, which is an orthogonal direction to our approach to select nodes in the target graph computed at each search step. (3) BIHYB [44] is a general framework with an upper-level RL agent to modify the graph and a lower-level heuristic algorithm for tasks such as Graph Edit Distance computation. However, the method is not tailored addressing the special challenges of Subgraph Matching.

2.3 Search-based methods for Subgraph Matching

Due to the NP-hard nature of Subgraph Matching, backtracking search is a naturally suitable algorithm since it exhaustively explores the solution space by starting with an empty match and adding one new node pair to the current match at each step. When the current match cannot be further extended, the search backtracks to its previous search state, and explores other node pairs to extend the match. However, naively enumerating all the possible states in the entire search space is intractable in practice, and there-

fore existing efforts mainly aim to reduce the total number of search steps for the backtracking search via mainly three ways [38]: (1) Filter nodes in G to obtain a small set of candidate nodes for each node in q as a pre-processing step before the backtracking search; (2) Order the nodes in q before the search; (3) Generate a local candidate set of nodes in each step of the search based on the current search state. Algorithm 1 summarizes the overall backtracking search based framework for Subgraph Matching. It is worth noting that the first three means correspond to the three steps in the algorithm, and therefore any improvement in any of the three steps can be regarded as orthogonal to each other.

Algorithm 1 Search-based Subgraph Matching.

- 1: **Input:** Query graph q , data graph G .
 - 2: **Output:** Matches from q to G .
 - 3: Filter: $C \leftarrow$ generate candidate node sets.
 - 4: Order: $\phi \leftarrow$ generate an ordering for V_q .
 - 5: Search: $\text{Backtracking}(q, G, C, \phi, \{\})$.
-

The basic idea of backtracking search is outlined in Algorithm 2. The recursive algorithm starts with an empty node-node mapping, and tries to add one new node pair to the mapping M at each recursive call. The action is the new node pair (u_t, v_t) , where $u_t \in V_q$ is selected according to the ordering ϕ , and $v_t \in V_G$ is selected according to a policy to be one of the local candidate nodes (line 8), that can be mapped to u_t . It is noteworthy that this local candidate node set “ $\mathcal{A}_{u_t} \subseteq V_G$ ” is refined over the global candidate sets C based on the current search state s_t , defined as (q, G) along with the current mapping M . and u_t whose details are non-trivial and explained in the supplementary material, since it ensures any node in \mathcal{A}_{u_t} would lead to the extended subgraphs at s_t still being isomorphic to each other. Thus, we regard the local candidate set \mathcal{A}_{u_t} for u_t as our action space, for which we learn a policy (line 9) to order the nodes, resulting in an ordered list $\mathcal{A}_{u_t, \text{ordered}}$.

Despite existing efforts to compute a small C , a good ϕ , and a small \mathcal{A}_{u_t} to reduce search space, we observe that the size of \mathcal{A}_{u_t} can be up to thousands of nodes for many real-world large target graphs, calling for a smarter policy to order the nodes not only in q but also in G (\mathcal{A}_{u_t} to be specific). To the best of our knowledge, all the existing methods adopt a random ordering, i.e. a $\mathcal{A}_{u_t, \text{ordered}}$, to select a node from \mathcal{A}_{u_t} . We conjecture it is because existing local candidate computation techniques can further prune nodes from C , and thus enumerating \mathcal{A}_{u_t} in a random ordering can be tractable on small graph pairs. We will experimentally show that this accounts for their failure to find a match for many large graph pairs. In fact, a theoretically perfect policy, policy^* , can find the entire match of the query graph in V_q steps or recursive calls, assuming q has at least one match with G . This again motivate our proposed method to improve the policy over \mathcal{A}_{u_t} .

Algorithm 2 Backtracking(q, G, C, ϕ, M)

```

1: Input:  $q, G, C, \phi$ , and current mapping  $M$ .
2: Output: Subgraph match mappings.
3: if  $|M| = |V_q|$  then
4:   output  $M$ ;
5:   return;
6: end if
7:  $u_t \in V_q \leftarrow \phi(M)$ ;
8:  $\mathcal{A}_{u_t} \leftarrow s_t.\text{getLocalCand}(u_t)$ ;
9:  $\mathcal{A}_{u_t, \text{ordered}} \leftarrow \text{policy}(s_t, \mathcal{A}_{u_t})$ ;
10: for  $v_t$  in  $\mathcal{A}_{u_t, \text{ordered}}$  do
11:    $M \leftarrow M.\text{add}(u_t, v_t)$ ;
12:   Backtracking( $q, G, C, \phi, M$ );
13:    $M \leftarrow M.\text{remove}(u_t, v_t)$ ;
14: end for

```

3 Proposed Method

In this section we formulate the problem of Subgraph Matching as learning an RL agent that grows the extracted subgraphs by adding new node pairs to the current subgraphs. N-BLS runs an inner MCTS simulation under each state of the outer backtracking search, resulting in a bi-level search framework. We first describe the environment setup, then depict our proposed encoder-decoder neural network which provides actions for our agent to grow the subgraphs in a search context. Finally, we describe how to tackle the sparsity of solutions in Subgraph Matching via bi-level tree search.

3.1 RL Formulation of Subgraph Matching

We formulate the Subgraph Matching problem as a Markov Decision Process (MDP), where the RL agent starts with an empty solution, and iteratively matches one node pair at a time until no more nodes can be matched. As mentioned in Section 2.3, our policy assigns a score to each action in \mathcal{A}_{u_t} , and therefore can be modeled as a policy network $P_\theta(a_t|s_t)$ that computes a probability distribution over \mathcal{A}_{u_t} for the current state s_t , where the node pair to select consists of (u_t, v_t) . However, since u_t is chosen by ϕ , we regard an action as a node v_t selected from \mathcal{A}_{u_t} . Since each action is a target node in \mathcal{A}_{u_t} , the neural network must learn good node embeddings that capture the current matching status in each search state, which will be shown in Section 3.2. We will also show that a value network $v_\theta(s_t)$ is needed to facilitate the training of $P_\theta(a_t|s_t)$ in Section 3.3. We describe the definition of reward in the rest of this section.

Since the entire q is desired to be matched with G , a key requirement of Subgraph Matching, we define the immediate reward of matching one new node pair as a function of the current subgraph size: $r = \exp(\alpha \frac{|S|+1}{|q|}) - \exp(\alpha \frac{|S|}{|q|})$, where $|S|$ denotes the number of nodes in $q[S]$ (or $G[S]$), $|q|$ denotes the number of nodes in q , and α is a hyperparameter controlling the slope of the reward curve. This

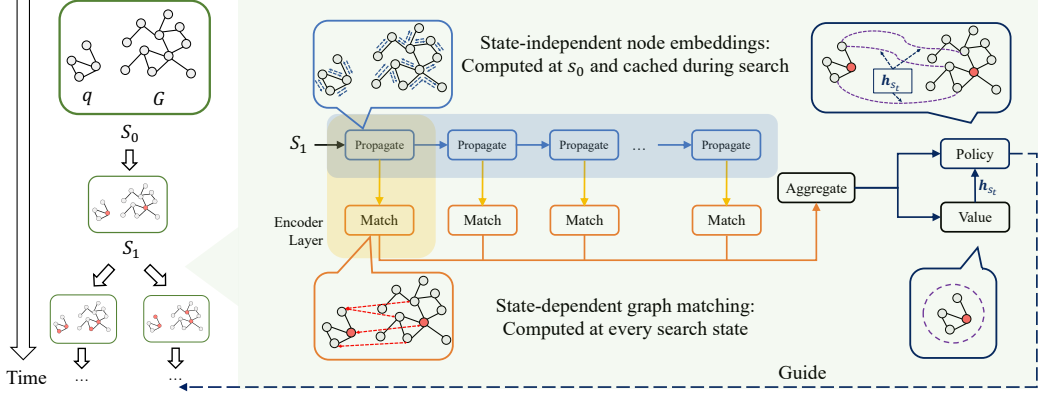


Figure 1: The overall process of Subgraph Matching is a bi-level search algorithm that matches one node pair at a time for the input query q and target graph G guided by a learned policy. Due to the large action space incurred by the large G in practice, we propose to train a policy network to guide the selection of local candidate nodes in G at each search state. This requires effective node embeddings to be learned that can reflect the node-to-node mapping at the current state and contribute to the prediction of the policy and reward. To achieve this end, we propose a novel QC-SGMNN encoder layer consisting of a “Propagation” module that performs intra-graph message passing as a typical GNN and a “Matching” module that performs state-dependent inter-graph matching (Section 3.2.1). A value network is also trained to facilitate the improvement of policy prediction under the Monte Carlo Tree Search self-play training framework (Section 3.3).

function starts by assigning a relatively small value initially when the partial solution is small, and encourages the RL agent to match more and more nodes towards larger solutions due to the exponential function. For simplicity, we define the accumulated reward function $\rho(s_t) = \exp(\alpha \frac{|S(s_t)|}{|q|})$, where $|S(s_t)| = |S_{t,q}| = |S_{t,G}|$ denotes the size of the matched subgraph at s_t . Under policy π , the value function is defined as $v_\pi(s_t) = \mathbb{E}_{\tau \sim \pi} [\sum_{j=0}^T \gamma^j r_{t+j+1} | s = s_t]$, where γ is the discount factor, and T denotes the total number of steps from s_t to a terminal state under π . In Subgraph Matching, the environment can be regarded as deterministic, i.e. s_{t+1} is determined based on s_t and a_t , and if we assume $\gamma = 1$, $v_\pi(s_t)$ can be simplified to $v_\pi(s_t) = \rho(s_T) - \rho(s_t)$, which intuitively reflects the eventual solution size starting from s_t .

3.2 Encoder-Decoder Design for Policy and Value Estimation

Our neural network consists of an encoder which produces node-level embeddings for V_q and V_G and a decoder which transforms the node embeddings into $P_\theta(a_t | s_t)$ and $v_\theta(s_t)$. We identify the following challenges: (1) Each state s_t consists of q , G , and the mapping M_t between the matched nodes $S_{t,q} \subseteq V_q$ and $S_{t,G} \subseteq V_G$, which should be effectively represented and utilized in predicting $v_\theta(s_t)$ and $P_\theta(a_t | s_t)$; (2) $P_\theta(a_t | s_t)$ is dependent on s_t and a_t , potentially requiring the node embeddings to be recomputed at every search step and incurring too much computational overhead; (3) Existing Graph Neural Networks (GNN) relying on message passing (e.g. [18, 42, 48]) are inherently local, which are incompatible with value and policy estimation requiring global matching of q to G . Even the more recent GNNs that enhance expressiveness beyond 1-Weisfeiler-Lehman test [29, 45] still cannot guarantee the capturing of nodes in the solution, since otherwise the NP-hard task would then be solved. This motivates the following design leveraging the properties of Subgraph Matching as much as possible.

3.2.1 Encoder: Embedding Generation via QC-SGMNN

The nodes of q and G are encoded into initial one-hot embeddings $\mathbf{h}^{(0)} \in \mathbb{R}^{|\Sigma|}$, and fed into K sequentially stacked Query-Conditioned Subgraph Matching Neural Networks (QC-SGMNN) layers to obtain $\mathbf{h}^{(K)} \in \mathbb{R}^D$, where D is the dimension of embeddings, followed by a JUMPING KNOWLEDGE [47] network to combine the node embeddings from the K layers to obtain the final node embeddings, denoted as “Aggregate” in Figure 1.

We start by observing that Subgraph Matching desires all nodes in q to be matched with G , and existing works in Subgraph Matching aiming at reduce \mathcal{A}_{u_t} (Section 2.3) guarantee no false pruning. In other words, \mathcal{A}_{u_t} is guaranteed to contain the solution nodes in G that should match with u_t , i.e. \mathcal{A}_{u_t} provides useful hints of which nodes should be matched together. We then compute the candidate space $\mathcal{A}_{u'}$ for every remaining query graph node $u' \notin S_{t,q}$, resulting in a mapping $M'_t = \{u' \mapsto \mathcal{A}_{u'}, \forall u' \in V_q \setminus S_{t,q}\}$. Intuitively, M'_t can be regarded as hints of *future* node-node mappings. In contrast, $M_t = \{u \mapsto \{v\}, \forall u \in S_{t,q}\}$ reflects the *current* state s_t , which maps each node in $S_{t,q}$ to a unique node in G . We define \tilde{M}_t as the union of M_t and M'_t , and define \tilde{M}_t^{-1} as the reverse mapping of \tilde{M}_t , which serve as the basis for the matching module.

QC-SGMNN consists of a propagation module, which performs regular intra-graph message passing on q and G individually, and a matching module, which performs state-dependent subgraph-graph matching leveraging \tilde{M}_t to pass information between q and G . Specifically,

$$\begin{aligned}
\mathbf{h}_{u,\text{intra}}^{(k+1)} &= f_{\text{agg}}(\{f_{\text{msg}}(\mathbf{h}_{u,\text{intra}}^{(k)}, \mathbf{h}_{u',\text{intra}}^{(k)}) | u' \in \mathcal{N}(u)\}), \\
\mathbf{h}_{v,\text{intra}}^{(k+1)} &= f_{\text{agg}}(\{f_{\text{msg}}(\mathbf{h}_{v,\text{intra}}^{(k)}, \mathbf{h}_{v',\text{intra}}^{(k)}) | v' \in \mathcal{N}(v)\}), \\
\mathbf{h}_{q,\text{intra}}^{(k+1)} &= f_{\text{readout}}(\{\mathbf{h}_{u,\text{intra}}^{(k+1)} | u \in V_q\}), \\
\mathbf{h}_{u,G \rightarrow q}^{(k+1)} &= f_{\text{agg}}(\{f_{\text{msg}}(\mathbf{h}_{u,\text{intra}}^{(k+1)}, \mathbf{h}_{v,\text{intra}}^{(k+1)}) | v \in \tilde{M}_t(u)\}), \\
\mathbf{h}_{v,q \rightarrow G}^{(k+1)} &= f_{\text{agg}}(\{f_{\text{msg}}(\mathbf{h}_{v,\text{intra}}^{(k+1)}, \mathbf{h}_{u,\text{intra}}^{(k+1)}, \mathbf{h}_{q,\text{intra}}^{(k+1)}) | u \in \tilde{M}_t^{-1}(v)\}), \\
\mathbf{h}_u^{(k+1)} &= f_{\text{combine}}(\mathbf{h}_{u,G \rightarrow q}^{(k+1)}, \mathbf{h}_{u,\text{intra}}^{(k+1)}), \\
\mathbf{h}_v^{(k+1)} &= f_{\text{combine}}(\mathbf{h}_{v,q \rightarrow G}^{(k+1)}, \mathbf{h}_{v,\text{intra}}^{(k+1)}).
\end{aligned} \tag{1}$$

The first two steps can be any intra-graph message passing GNNs such as Graph Attention Networks [42] with a message function f_{msg} and an aggregation function f_{agg} , corresponding to the propagation module. The middle three steps compute intermediate embeddings that will be used for the last two steps, i.e. the matching module. Specifically, $\mathbf{h}_{u,G \rightarrow q}^{(k+1)}$ and $\mathbf{h}_{v,q \rightarrow G}^{(k+1)}$ compute the cross-graph message passing from G to q and q to G using \tilde{M}_t and \tilde{M}_t^{-1} , respectively (represented as the red dashed lines in Figure 1). A graph-level embedding $\mathbf{h}_{q,\text{intra}}^{(k)}$ is computed via f_{readout} and used in the information passing from q to G to let the embeddings of V_G query-conditioned. We do not inject the graph-level embeddings of G into $\mathbf{h}_{u,G \rightarrow q}^{(k+1)}$, since the large size of G could result in too much information loss in the readout operation. The last two steps combine the intra-graph embeddings and inter-graph embeddings via f_{combine} to produce the final output embeddings. It is noteworthy that f_{msg} and f_{agg} refer to the general class of functions that yield messages between two nodes and performs aggregation on a set of messages, and in practice, the propagation and matching modules can use different functions for f_{msg} and f_{agg} .

To address challenge (2), we make the observation that $\mathbf{h}_{\text{intra}}^{(k)}$ only depends on q and G and is independent of M_t , and thus can be computed once and cached at the beginning of the search (denoted as the top branch in Figure 1) and later reused throughout the search. Our QC-SGMNN decouples the propagation and matching steps and outputs two sources of information separately, allowing the search to cache the state-independent node embeddings and dynamically select the computational paths during search. Thanks to the caching, only the initial iteration requires the $\mathcal{O}(|E_q| + |E_G|)$ computation, and all the subsequent iterations only involve $\mathcal{O}(|V_q| |\bar{\mathcal{A}}_{u_t}|)$ complexity, where $|\bar{\mathcal{A}}_{u_t}|$ is the average size of local candidate space.

3.2.2 Decoder: $v_\theta(s_t)$ and $P_\theta(a_t|s_t)$ Estimation

Since the node embeddings of q has received the right amount of information from \tilde{M}_t , we propose an attention-based mechanism to compute the value: $v_\theta(s_t) = \text{MLP}(\mathbf{h}_{s_t}) = \text{MLP}(\sum_{u \in V_q} f_{\text{att}}(\mathbf{h}_u, \{\mathbf{h}_{u'} | u' \in V_q\}) \mathbf{h}_u)$, where f_{att} computes one attention score per node normalized across V_q to tackle challenge (3). Intuitively, the attention function learns which nodes are important for contributing to the eventual subgraph selected by s_T . Due to the cross-graph communication in QC-SGMNN, we only aggregate nodes from V_q to obtain the state representation \mathbf{h}_{s_t} , taking advantage of the fact that $|V_q|$ is typically much smaller than $|V_G|$ in Subgraph Matching, further addressing challenge (2).

For the policy, we again aim to tackle challenge (3), by reusing \mathbf{h}_{s_t} . The reasons are two-fold. First, by definition $P_\theta(a_t|s_t)$ requires s_t as input; Second, the attention mechanism used to compute \mathbf{h}_{s_t} capturing the future subgraph. Combined with a bilinear tensor product with learnable parameter $\mathbf{W}^{[1:F]} \in \mathbb{R}^{D \times D \times F}$ with a hyperparameter F to allow the action node embeddings \mathbf{h}_{u_t} and \mathbf{h}_{v_t} to fully interact, we obtain $P_{\text{logit}}(a_t|s_t) = \text{MLP}(\text{CONCAT}(\mathbf{h}_{u_t}^T \mathbf{W}^{[1:F]} \mathbf{h}_{v_t}, \mathbf{h}_{s_t}))$, followed by a softmax normalization over the logits for all the actions. The decoder has time complexity $\mathcal{O}(|V_G| + |\bar{\mathcal{A}}_{u_t}|)$.

3.3 Addressing Reward Sparsity via Monte Carlo Tree Search (MCTS)

To address the reward sparsity issue mentioned in Section 1, we adopt the Monte Carlo Tree Search (MCTS) method [6, 19] used in AlphaZero [35] and MuZero [33] as an additional step to improve the raw policy predicted by a neural network. We conjecture MCTS helps alleviating the reward sparsity issue due to its ability to spend additional computation at each s_t to further explore and revise $P_\theta(a_t|s_t)$, and provide a better search policy π based on the visiting counts associated with each state. We thus let N-BLS perform MCTS at each search step during training. Since MCTS naturally expands s_t into a search tree below it, by performing MCTS at each s_t , we obtain a bi-level search framework where the outer level is the backtracking search, which always selects a new node pair to match, and the inner level is the MCTS, which allows revisiting states and providing an improved search policy π used for training $P_\theta(a_t|s_t)$. We only use the outer search during inference to make it as fast as possible.

We find for our task, the varying number of actions per state causes insufficient exploration for states with a large action space, while too much exploration for states with a small action space. We propose to dynamically compute how many MCTS iterations to perform for each state based on the action space size, $|\mathcal{A}_{u_t}|$, using $\min(\omega|\mathcal{A}_{u_t}|, \text{max_iters})$. In other words, the amount of MCTS iterations allocated for each state during training is proportional to the action space size bounded by a pre-defined maximum number of iterations allowed, `max_iters`. More details can be found in the supplementary material.

In order to utilize MCTS, a value network $v_\theta(s_t)$ needs to be designed to facilitate the selection step of each MCTS iteration. Initially, it is unlikely that the untrained $v_\theta(s_t)$ and $P_\theta(a_t|s_t)$ lead to a large reward $v_\pi(s_t)$ by following π , but since the reward is used to train $v_\theta(s_t)$, in subsequent training epochs, the improved $v_\theta(s_t)$ can guide MCTS to find better π , and thus a better $P_\theta(a_t|s_t)$. Overall, both the policy and value networks are trained under the self-play framework. More explanations and intuitions can be found in the supplementary material. We use the loss function in [36] to train $P_\theta(a_t|s_t)$ and $v_\theta(s_t)$: $L = (v_\pi(s_t) - v_\theta(s_t))^2 - \pi^T \log(\mathbf{P}) + c \|\boldsymbol{\theta}\|^2$, where c is a hyperparameter for weight regularization and $\boldsymbol{\theta}$ denotes the parameters of our model.

4 Experiments

We evaluate N-BLS against five backtracking-based algorithms for exact Subgraph Matching, and conduct experiments on five real-word target graphs from various domains, whose details can be found in the supplementary material. We find N-BLS written in Python can outperform the state-of-the-art solver written in C++ under most cases, suggesting the effectiveness of the learned policy for ordering nodes in G . Code, trained model, and all the datasets used in the experiments are released as part of the supplementary material for reproducibility. More results and the ablation study can be found in the supplementary material.

4.1 Datasets and Evaluation Protocol

We use five large real-world target graphs provided by a recent survey paper that consistently compares several Subgraph Matching solvers [38]. For each G , we generate three query sets for testing, each with 100 randomly sampled query graphs of 32, 64, and 128 nodes, denoted as “ Q_{32} ”, “ Q_{64} ”, and

Table 1: Datasets description.

Dataset	Domain	$ V_G $	$ E_G $
HUMAN	Biology	4,674	86,282
HPRD	Biology	9,460	34,998
DBLP	Social	317,080	1,049,866
EU2005	Web	862,664	16,138,468
YOUTUBE	Social	1,134,890	2,987,624

Table 2: Results on Subgraph Matching over five datasets each with three query sets. The ratio of the number of solved pairs over the 100 pairs per target graph is reported.

Dataset	QUICKSI	GRAPHQL	CECI	DP-ISO	HYBRID	NMATCH	N-BLS
HUMAN Q_{32}	1.00						
HUMAN Q_{64}	0.07	0.19	0.07	0.06	0.10	1.00	0.99
HUMAN Q_{128}	0.02	0.02	0.00	0.00	0.02	0.32	0.43
HPRD Q_{32}	0.52	0.53	0.65	0.55	0.70	0.90	0.99
HPRD Q_{64}	0.02	0.06	0.06	0.25	0.06	0.06	0.59
HPRD Q_{128}	0.00	0.00	0.00	0.00	0.00	0.00	0.00
DBLP Q_{32}	0.74	0.43	0.89	0.64	0.70	1.00	1.00
DBLP Q_{64}	0.40	0.14	0.59	0.44	0.29	0.71	0.97
DBLP Q_{128}	0.07	0.02	0.18	0.16	0.04	0.04	0.58
EU2005 Q_{32}	0.24	0.06	0.22	0.26	0.18	0.82	1.00
EU2005 Q_{64}	0.02	0.00	0.02	0.03	0.01	0.26	0.63
EU2005 Q_{128}	0.01	0.01	0.01	0.01	0.01	0.01	0.21
YOUTUBE Q_{32}	0.35	0.24	0.40	0.38	0.53	0.41	0.78
YOUTUBE Q_{64}	0.26	0.23	0.37	0.36	0.24	0.10	0.90
YOUTUBE Q_{128}	0.04	0.02	0.04	0.10	0.02	0.00	0.11

“ Q_{128} ”, respectively, resulting in 100 (q, G) graph pairs. As shown in Table 1, the largest target graph, YOUTUBE, has over 1M nodes and 2M edges.

To train our model, due to the self-play framework, we can sample query graphs of any sizes and simply let N-BLS perform the proposed bi-level search algorithm and collect training data from the search tree. Therefore, we sample query graphs from each target graph of sizes ranging from 4 nodes to 128 nodes, and validate that no query graph in the testing set is visible to the model, that is, no graph in the training set is isomorphic to any graphs in the testing set. During the testing stage, for each target graph, we use the following evaluation protocol. For each graph pair, we set a time limit of 5 minutes, and record the result of whether a solution is found or not, and then average across the 100 pairs for each target graph.

4.2 Baselines and Parameter Settings

We compare N-BLS against a series of baseline solvers written in C++ whose source codes are provided by [38]: QUICKSI [34], GRAPHQL [12], CECI [3], DP-ISO [10], and HYBRID [38]. For HYBRID, we follow the recommendation by the authors of [38] by using DP-ISO for filtering, GRAPHQL for query node ordering, and LFTJ [41, 39] for local candidate computation. We also include NMATCH [26] as a learning-based method for exact Subgraph Matching, by adapting the original implementation provided by the authors of [26] into our backtracking search framework. Specifically, at each search step, we invoke the inference step of the released trained NMATCH model over the input graphs, and obtain a matching score for each (u_t, v_t) action node pair to guide the selection of nodes in \mathcal{A}_{u_t} .

Since we are among the first to learn a policy for selecting nodes in G , we use DP-ISO for filtering and GRAPHQL for query node ordering. We implement the backtracking search framework and DP-ISO’s local candidate computation algorithm in Python. N-BLS uses 4 layers of the proposed QC-SGMNN encoders. ω is set to 10 and `max_iters` is set to 120. Training is performed on a server with NVIDIA Tesla V100 GPUs. We train N-BLS for 2 days with the Adam optimizer [17] and initial learning rate 0.001.

4.3 Results

As shown in Table 6, N-BLS achieves the same or better performance on 14 out of 15 query sets, across a variety of query graph sizes, target graph sizes, graph densities, and domains. We observe baseline solvers fail completely on many Q_{128} and Q_{64} query sets, as search space pruning on its own is not effective enough to guarantee solutions in such cases. Learning-based methods outperform solver baselines because they provide a better target graph node ordering, under the same search framework. Out of the learning-based methods, N-BLS consistently outperforms NMATCH, as it features a more powerful encoder that efficiently computes a policy conditioned on the current search state with a better inter-graph communication mechanism. This also suggests that the target

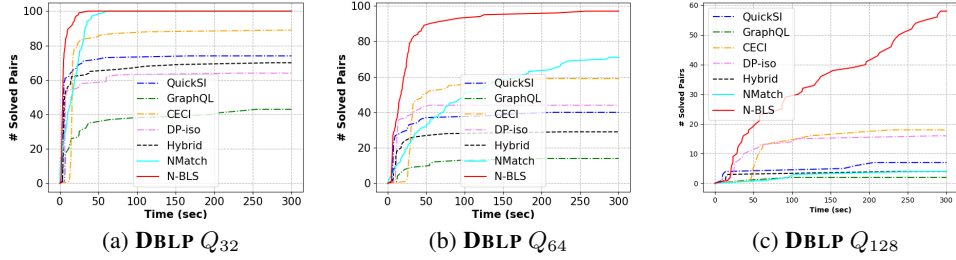


Figure 2: Comparison of the curves of the number of solved pairs versus time on DBLP.

graph node ordering provided by N-BLS is much better than the random ordering adopted by solver baselines, confirming that our novelties indeed greatly improve Subgraph Matching performance.

We observe that when the query graph size increase, all methods show lower performance, which can be attributed to the exponentially growing search space. It is noteworthy that the survey paper comparing existing solvers [38] uses query graphs up to 32 nodes, whereas we challenge all methods by testing on query graphs up to 128 nodes. The fact that N-BLS is able to solve more graph pairs than baselines when the query graphs contain 128 nodes demonstrates good scalability of N-BLS.

On HPRD Q_{32} , although NMatch is able to solve 1 more pair than N-BLS, the fact that NMatch is also a learning-based model and it outperforms the non-learning solvers suggests the effectiveness of using learning to select nodes in the target graph G . It is also worth noting that all methods fail to solve any pair on HPRD Q_{128} . A recent work [28] studying when Subgraph Matching is difficult empirically discovers that sometimes small query and target graphs may also be hard to solve. Such hard instances can be identified using a phase transition plot, where the difficulty of different graph pairs is visualized by running a Subgraph Matching solver on many randomly generated graph pairs with varying edge probabilities. However, how to estimate the difficulty of a given graph pair without running a solver remains an open question. Regardless of how to locate such difficult graph pairs, we still verify the usefulness of learning-based approaches. N-BLS can be beneficial not only on large target graphs, but also smaller target pairs that existing algorithms struggle to solve. We indeed see this trend on HUMAN Q_{128} , the smallest of the 5 target graphs, where baselines fail to solve few if any graph pairs and N-BLS solves many. This suggests our model can enable Subgraph Matching applications on previously unattainable datasets.

4.4 Visualization of Performance across Time

To examine the efficiency of each method and further analyze the efficacy across time, we conduct the following experiment. For each (q, G) pair, we record the time the method takes to find a solution, and accumulate the number of solved pairs across time. From $t = 0$ to $t = 300$ seconds, an increase at t indicates the method solves one graph pair at t . The earlier a method reaches 100 pairs, the faster and better the method is. As seen in Figure 2, N-BLS runs fast on Q_{32} and takes more time on Q_{64} and Q_{128} to solve a pair, but consistently outperforms baselines at the end of 5 minutes, demonstrating the efficiency of N-BLS in practice.

In theory, given an infinite amount of time, every method adopting the backtracking search algorithm would be able to solve a graph pair. However, such assumption is not practical. Thus, the curves in Figure 2 have the practical implication that under a reasonable amount of time budget, the idea of using a smarter policy indeed brings better performance to Subgraph Matching. Another observation is that the baseline solvers flatten towards the end of 5 minutes, indicating that they get stuck in unpromising search states that are unlikely to contain the solution, confirming the severity of the aforementioned challenges of solution and reward sparsity. It is worth noting that N-BLS on Q_{128} continues to solve more pairs towards the end of 5 minutes, suggesting that further improvement may be achieved if N-BLS is implemented in C++ with optimization.

5 Conclusion

In this paper, we tackle the challenging and important task of Subgraph Matching, and present a new method for efficient and effective exact Subgraph Matching. It contains a novel encoder-

decoder neural network architecture trained under by adopting the Monte Carlo Tree Search (MCTS) algorithm for self-play to improve the policy and value estimation. The core component, QC-SGMNN, is a query-conditioned graph encoder that performs intra-graph propagation and inter-graph node matching to capture each state. To address the reward sparsity issue posed by the large action space, we perform MCTS at each search iteration to obtain more reliable training signals. We experimentally show the practical usefulness of the proposed N-BLS method on the important Subgraph Matching task. Specifically, N-BLS is able to solve more graph pairs than several existing Subgraph Matching solvers on five large real-world datasets.

A Details on Training of N-BLS

A.1 Details on Bi-Level Tree Search

We outline the entire bi-level search framework in Algorithm 3. The goal of the bi-level tree search is to leverage MCTS as an inner search step (lines 10-21) to provide an improved search policy π (line 22) which is used to select a node from the local candidate space \mathcal{A}_{u_t} (line 23). Since the bi-level search framework is used to provide training signals, the search tree \mathcal{T} is the output. We will describe how to collect training signals from \mathcal{T} in Section A.2.

In each MCTS iteration (lines 11-20), there are three steps.

(1) Select. The algorithm starts with the current node and successively selects child nodes until a leaf node is reached, where a leaf node is either a node that cannot be further expanded, i.e. a node with an empty action space, or a node that has not been visited according to the search tree \mathcal{T} that maintains all the nodes that have been visited. Each selection process looks at all the possible actions associated with the current node `child_node`, i.e. state s_t , and selects a child node, i.e. a next state s_{t+1} , with the maximum upper confidence bound (UCB). Each search tree node stores an accumulated reward and a visiting count both initialized to 0. We denote the reward associated with each outgoing edge (s_t, a_t) as $W(s_t, a_t)$, which is obtained by looking up the reward associated with the next state s_{t+1} by executing a_t . Similarly, we denote the visiting count associated with each action as $N(s_t, a_t)$ which is obtained by looking up the next state’s visiting count. The UCB can then be computed as,

$$Q(s_t, a_t) + U(s_t, a_t) = \frac{W(s_t, a_t)}{N(s_t, a_t)} + c_{\text{puct}} P_{\theta}(a_t|s_t) \frac{\sqrt{\sum_{a'_t \in \mathcal{A}_{u_t}} N(s_t, a'_t)}}{1 + N(s_t, a_t)}, \quad (2)$$

where c_{puct} is a hyperparameter controlling the level of exploration, i.e. the U term. It is noteworthy that due to the balanced exploitation and exploration, MCTS is allowed to re-select actions that have been selected by previous MCTS iterations. Such re-visitation allows MCTS to update their visiting count and accumulated rewards (the backup step below), which can result in an improved search policy to train the policy network. In contrast, the outer search, i.e. the backtracking search, always selects a new node that has not been selected (line 23 only selects from \mathcal{A}_{u_t} which is updated at line 27), which allows the inner MCTS to restart from different nodes (line 11) at different search steps, and is a desirable behavior for quickly exploring as many new states as possible to find solutions. Figure 3 illustrates the process. Thus, during training, the outer backtracking search and the inner MCTS can be mutually beneficial to each other, and during inference, we only use the backtracking search with the trained policy network to obtain an ordered action space $\mathcal{A}_{u_t, \text{ordered}}$ (line 9 of Algorithm 1 in the main text) for efficiency.

Algorithm 3 $\text{Search_bilevel}(q, G, C, \phi, M, \mathcal{T})$ for training N-BLS.

```

1: Input:  $q, G, C, \phi$ , the current mapping  $M$ , and the search tree  $\mathcal{T}$ .
2: Output:  $\mathcal{T}$  for training signals.
3: if  $|M| = |V_q|$  then
4:   return;
5: end if
6:  $u_t \in V_q \leftarrow \phi(M)$ ;
7:  $\mathcal{A}_{u_t} \leftarrow s_t.\text{getLocalCand}(u_t)$ ;
8: while  $\mathcal{A}_{u_t}$  is not empty do
9:   num_iters  $\leftarrow \min(\omega|\mathcal{A}_{u_t}|, \text{max\_iters})$ ;
   // Inner MCTS.
10:  for  $i$  in  $\text{range}(\text{num\_iters})$  do
11:    cur_node  $\leftarrow \mathcal{T}.\text{getCurNode}()$ ;
    // MCTS: (1) Select.
12:    while cur_node is not a leaf node do
13:      Select child_node:  $\arg \max(Q + U)$  according to Equation 2;
14:       $\mathcal{T}.\text{addEdge}(\text{cur\_node}, \text{child\_node})$ ;
15:      cur_node  $\leftarrow \text{child\_node}$ ;
16:    end while
    // MCTS: (2) Expand and evaluate.
17:    if cur_node has a non-empty action space then
18:      Compute  $P_\theta$  for all the actions of cur_node and  $v_\theta$  of cur_node;
19:    end if
    // MCTS: (3) Backup.
20:    Increment  $N$  by 1 and update  $W$  by  $v_\theta$  of each node from cur_node to  $\mathcal{T}.\text{root\_node}$ ;
21:  end for
22:  Compute  $\pi$  of  $\mathcal{T}.\text{getCurNode}()$  according to Equation 3;
23:  Sample the action node  $v_t \in \mathcal{A}_{u_t} \sim \pi$ ;
24:   $M \leftarrow M.\text{add}(u_t, v_t)$ ;
25:   $\text{Search\_bilevel}(q, G, C, \phi, M, \mathcal{T})$ ;
26:   $M \leftarrow M.\text{remove}(u_t, v_t)$ ;
27:   $\mathcal{A}_{u_t} \leftarrow \mathcal{A}_{u_t}.\text{remove}(v_t)$ ;
28: end while

```

(2) Expand and evaluate. We follow AlphaGo Zero [36] by not performing any rollouts. Instead, we expand the leaf node by computing the policy associated with all the outgoing edges, i.e. actions associated with the leaf node, as well as evaluating the value associated with the leaf node (line 18). Such strategy allows fast expansion and evaluation without the need to perform any sequential rollouts.

(3) Backup. We update the visiting count and accumulated reward by following the parent pointer successively, starting from the current leaf node and ending at the root node of \mathcal{T} . In AlphaGo Zero, the backup step ends at the current node $\mathcal{T}.\text{getCurNode}()$, since the Go game is intrinsically sequential, and thus subsequent steps that reuse the search tree will not backtrack to an earlier state that is higher than $\mathcal{T}.\text{getCurNode}()$ in the tree. In other words, the game will always move on without the possibility for one player to regret and backtrack to an earlier state. In contrast, our Subgraph Matching naturally requires search, and in a later search

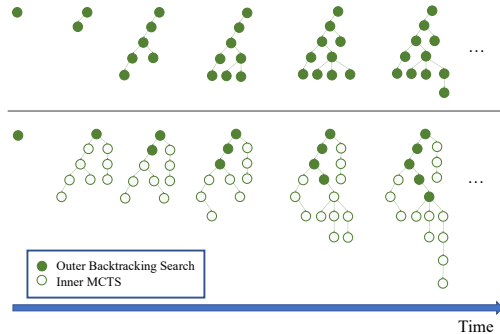


Figure 3: Comparison between the backtracking search (top) and the bi-level search (bottom). For clarity, we omit the details of MCTS, e.g. the selection step, the expansion step, etc., and use different patterns to denote search tree nodes generated by the inner MCTS and the nodes visited by the outer backtracking search. Across time, the search tree grows, and for simplicity, we do not ensure equal number of tree node increase between consecutive trees.

step, the outer search may backtrack to an earlier state that is higher than $\mathcal{T}.getCurNode()$ in the tree. Therefore, we backup N and W all the way back to the root of the tree to allow future MCTS steps to reuse such statistics to help finding the improved search policy π which is described next.

After the MCTS iterations, we compute π as follows:

$$\pi(a_t|s_t) = \frac{N(s_t, a_t)^{1/\tau}}{\sum_{a'_t \in \mathcal{A}_{u_t}} N(s_t, a'_t)^{1/\tau}}, \quad (3)$$

where τ is a hyperparameter controlling the temperature: A higher temperature causes π to be closer to a uniform probability distribution allowing more exploration, while a lower temperature causes π to be closer to a one-hot vector, i.e. intuitively more trust is placed on the visiting count to guide the search.

A.2 Details on Collecting Training Signals

For AlphaGo Zero [36], the value and policy network training signal is collected for each outer search state, as defined in Section A.1. The value network training signals are collected by executing the policy π until the end of the game, and observing the winning or losing of the game, denoted as z , which is set to +1 or -1. z is assigned as the ground truth value to all outer search states of both the loser and winner.

In contrast, due to the combinatorial nature of Subgraph Matching, N-BLS collects training signals by simply examining all the search tree nodes of \mathcal{T} after performing the bi-level search for a given time budget which is set to 5 minutes for each training graph pair. For each outer search state, s_t , we assign the maximum accumulated reward obtained among all its children, s_{t+1} , plus the reward transitioning to that child as the ground truth value, z , of that outer search state. This definition gives N-BLS a more fine grained ground truth value compared to AlphaGo Zero.

In both AlphaGo Zero and N-BLS, the policy network training signals are collected from the visiting counts collected during each Monte Carlo Tree Search, where the ground truth policy of a search state is defined in Equation 3. After a ground truth policy and value are assigned, the state along with the true policy and value is pushed to a replay buffer that is sampled after each training iteration.

It is noteworthy that we view our method as being trained under a self-play [36, 9] framework, because after each round of learning, we evaluate both the current best model and the learned model on a sub-sample of 5 query graphs from the validation dataset, keeping the better performing model for the next iteration of learning. Intuitively, during training, our trained model at iteration i competes against the best copy of the trained, and the one that performs better on the validation set becomes the best model for the subsequent training process.

Comparison between the proposed Bi-Level Search and previous works adopting MCTS

Monte Carlo Tree Search has seen much success in many discrete-time discrete-action problems, such as in Go [35] and video games [30], making it a natural fit for Subgraph Matching. Unlike previous methods adopting Monte Carlo Tree Search, which stop playing the game after reaching a terminal state, our search can backtrack at any time to continue finding a solution. This dictates a need for a bi-level search framework, where an inner Monte Carlo Tree Search provides a good training signal for every outer search state, and an outer backtracking search can simulate the inference time search process, such that states with reward signals collected during training are useful during inference. This is in contrast to past works that cannot backtrack during inference time.

A subtler difference is in the motivation of adopting MCTS. MCTS has been traditionally viewed as a popular decision-time time planning algorithm [37], which can provide a better local policy at both the training and inference stages to guide the RL agent towards more promising states. In our task, this translates to MCTS may lead the outer backtracking search to find solutions for Subgraph Matching quickly, addressing the solution sparsity issue. However, in experiments, we observe that the selection step of MCTS may lead to certain states being visited repeatedly, which can negatively impact the number of explored states of N-BLS. Thus, we turn off MCTS during inference, and motivate the adoption of MCTS during training, to provide more reliable signals with the trade-off between speed and accuracy more justified in the training stage. In other words, we adopt MCTS into the proposed bi-level search framework for addressing the reward sparsity issue to train $P_\theta(a_t|s_t)$ and $v_\theta(s_t)$.

A.3 Details on Training Graph Pairs

For each target graph, we sample query graphs of various sizes to perform curriculum learning, as shown effective by earlier graph matching works [2, 26]. On HPRD, DBLP, EU2005, and YOUTUBE, the query graphs come in the following sizes: 4 nodes, 8 nodes, 16 nodes, 24 nodes, 32 nodes, 64 nodes, and 128 nodes. On HUMAN, the sizes are 20 nodes, 32 nodes, 64 nodes, and 128 nodes. We sampled 50 graphs from each of the 3 largest query graph sets and 5 graphs from each of the remaining 1-4 smaller query graph sets for training. On EU2005, we sample a 50,000 node subgraph from the whole target graph and use it as the target graph during training for efficiency. We still conduct testing on the whole 862,664-node 16,138,468-edge EU2005 target graph.

Before the encoder, we set the initial 16-dimensional node features to a learnable linear transformation of the local degree profile [7] concatenated with a 2-dimensional one-hot vector indicating whether a node is currently selected or not.

A.4 Details on Hyperparameters

For the encoder, we set the intra-graph f_{agg} and f_{msg} functions to GATv2 [5], and set the inter-graph f_{agg} function to be SUM and f_{msg} function to be dot-product style attention [40] over incoming messages. Specifically, the message collected by each query node, $\mathbf{h}_{u,G \rightarrow q} \in \mathbb{R}^D$, consists of attended node embeddings from $v' \in \tilde{M}_t(u)$. Overall, $\mathbf{h}_{u,G \rightarrow q}$ is computed as

$$\sum_{v' \in \tilde{M}_t(u)} \text{softmax}_{v' \in \tilde{M}_t(u)} (\text{MLP}_q(\mathbf{h}_{u,\text{intra}})^T \text{MLP}_G(\mathbf{h}_{v',\text{intra}})) \text{MLP}_{\text{VAL},q}(\mathbf{h}_{v',\text{intra}}). \quad (4)$$

The message collected by each target node, $\mathbf{h}_{v,q \rightarrow G} \in \mathbb{R}^{2D}$, consists of attended node embeddings from $u' \in \tilde{M}_t^{-1}(v)$ and the whole query graph embedding, $\mathbf{h}_{q,\text{intra}}$. Overall, $\mathbf{h}_{v,q \rightarrow G}$ is computed as

$$\mathbf{h}_{v,q \rightarrow G} = \sum_{u' \in \tilde{M}_t^{-1}(v)} \text{CONCAT}(\mathbf{h}'_{v,q \rightarrow G}, \mathbf{h}_{q,\text{intra}}), \quad (5)$$

where

$$\mathbf{h}'_{v,q \rightarrow G} = \text{softmax}_{u' \in \tilde{M}_t^{-1}(v)} (\text{MLP}_q(\mathbf{h}_{u',\text{intra}})^T \text{MLP}_G(\mathbf{h}_{v,\text{intra}})) \text{MLP}_{\text{VAL},G}(\mathbf{h}_{u',\text{intra}}). \quad (6)$$

In total, we use four different MLPs, i.e. MLP_q , MLP_G , $\text{MLP}_{\text{VAL},q}$, and $\text{MLP}_{\text{VAL},G}$ following [40], with an ELU(\cdot) activation after the final layer.

We set the f_{combine} function to be the concatenation CONCAT followed by MLP. We choose MEAN as the readout function f_{readout} for computing the query graph-level embedding. We choose the MAX function as the aggregation function for our Jumping Knowledge network which aggregates the node embeddings. We apply layer normalization [1] to the final node embeddings before feeding into the decoder. In the decoder, we found the recently proposed normalized attention [32] performs particularly well in f_{att} , which we denote by the function, $\xi(\cdot)$:

$$v_\theta(s_t) = \text{MLP}_v \left(\sum_{u \in V_q} \xi(\text{MLP}_{\text{att}}(\mathbf{h}_u)) \mathbf{h}_u \right) \quad (7)$$

For the encoder, we stack 4 layers of intra-graph message passing with dimension 16. We stack 4 layers of the inter-graph message passing with all MLPs outputting dimension 16. For the decoder, we set MLP_{att} to dimensions [16, 4, 1] and MLP_v to dimensions [16, 32, 16, 8, 4, 1]. We set the policy head’s bilinear layer, $\mathbf{W}^{[1:F]}$, to output dimension $F = 32$ and the policy head’s MLP to dimensions [48, 32, 16, 8, 1]. For all the MLPs, we use the ELU(x) activation function on the hidden layers. For MLP_v , we apply a LeakyReLU(\cdot) function following the final layer.

With respect to the bi-level search, we set the temperature τ to 5.0, max_iters to 120, ω to 10.0, and c_{puct} to 10.0. With respect to the reward function, we set α to 100 and γ to 1.0. Our replay buffer is of size 128. During the training process, we repeatedly run 5 minutes of bi-level search, populating the replay buffer, 3 minutes of replay buffer sampling and back propagation, training on as many replay buffer samples as possible, and 200 search iterations of “self-play” to choose whether or not we commit the learned model. One iteration of this process typically takes around 10 minutes. Hyperparameters were found by tuning for performance manually against the validation dataset.

B Notes on Search

B.1 Induced vs Non-Induced Subgraphs

One key detail regarding the subgraph definition is whether the subgraph is induced or non-induced. An induced subgraph $q[S]$ consists of all the nodes $S \subseteq V_q$ and requires that for every edge $(u, u') \in E_q$, if both u and u' are in S , then the edge (u, u') must be included in the edges of $q[S]$ as well. Intuitively, an induced subgraph does not allow any edges in the original graph to be dropped, as long as both endpoints of the edge are included by the subgraph. In contrast, a non-induced subgraph $q[S]$ consists of all the nodes $S \subseteq V_q$ but allows edges in E_q to be dropped. In this paper, we adopt the definition of non-induced subgraph, which is consistent with [10].

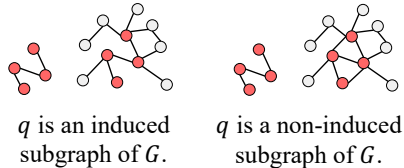


Figure 4: Comparison between an induced (left) and a non-induced (right) subgraph. We use the red color to denote the nodes that are included in the match.

B.2 Choice of Filtering, Query Node Ordering, and Local Candidate Computation

Motivated by prior work benchmarking solver baselines [38], we adopt HYBRID’s choice of filtering, query node ordering, and local candidate computation in N-BLS. As shown by the experimental results in the main paper, this design choice plays a much smaller role in Subgraph Matching than smart target graph node ordering, highlighting the need for N-BLS. Furthermore, we find that optimal filtering, query node ordering, and local candidate computation settings are highly dataset-dependent and hard to determine beforehand; however, because N-BLS’s design is orthogonal to such choices, it could easily be adapted to different filtering and query node ordering algorithms. We leave such study to future work.

The filtering method produces a global candidate set, $C : V_q \rightarrow V_t$, to drastically prune the search space of possible matchings. A simple method to compute C is to only allow mappings from u_t to v_t if v_t has degree higher than or equal to the degree of u_t . Different filtering algorithms use different such rules [38]. The query node ordering gives a search plan on which u nodes to select first. A simple method is picking the u nodes with the least candidate target nodes given by C . Different node ordering algorithms use different such rules [38].

During the search process, the local candidate set guarantees all subgraph mappings found throughout the search process are isomorphic. Specifically, it ensures u_t is matchable to v_t , i.e. $v_t \in \mathcal{A}_{u_t}$ only if (1) all edges between u_t and the currently matched query subgraph (with node set S) exist between v_t and the currently matched target subgraph: $(u_t, u') \in E_q, u' \in S \implies (v_t, M(u')) \in E_G$ and (2) the matching, (u_t, v_t) exists in the candidate set: $v_t \in C(u_t)$. There are many different implementations and optimizations to ensure these conditions hold. For instance, a query tree data structure [10] can be stored, allowing $O(1)$ lookup for $(u_t, u') \in E_q$ connections given a particular query node ordering. Different local candidate computation algorithms use different such optimizations [38]. Even though the subgraph isomorphism constraint is ensured through the local candidate set, Subgraph Matching is by no means an easy task due to the large amount of nodes in \mathcal{A}_{u_t} .

Among different techniques to further improve the accuracy of Subgraph Matching approaches, learning a state-dependent policy to select nodes from q is one direction worth mentioning. We currently only learn to select nodes in $\mathcal{A}_{u_t} \subseteq V_G$ partly because there is usually a small amount of nodes in q , e.g. 32 nodes or 128 nodes, while the number of nodes in \mathcal{A}_{u_t} is much larger as shown in Figure 8. As mentioned in the main text, RL-QVO [43] learns a state-independent node ordering policy, ϕ , via RL that is executed before search. We call such ϕ query node ordering. We argue it is a promising future direction to explore learning to select both nodes in q and nodes in G at each search iteration.

As shown effective by previous works, we adapt a promise-based search strategy [2], which backtracks to any earlier search state, instead of the immediate parent, whenever a terminal state is reached. We choose which earlier search state to backtrack to by computing a 2:1 weighted average of the search depth normalized by the query graph size and the percentage of explored actions, allowing search to quickly exit local minima. We include this adaptation on all learning methods. We also tried

the promise-based search on the solver baselines, but found the performance difference is minimal, typically around 2%. This is because solver baselines do not assign any ordering to the target graph nodes, thus there is no clear incentive to backtracking early.

C Comparison with Maximum Common Subgraph (MCS) Detection

Subgraph Matching and MCS detection are highly related tasks, and one can convert Subgraph Matching to MCS detection by feeding the input (q, G) pair to an MCS solver, and check if the MCS between q and G is identical to q . However, we note the following differences at the task level:

1. Subgraph Matching requires all the nodes and edges in q to be matched with G , whereas MCS detection does not require one of two input graphs to be contained in another.
2. Subgraph Matching by definition requires q to be smaller or equal to G , since otherwise the solver can immediately return “no solution”. In practice, the query graph is usually given by the user as input, and usually contains less than 100 nodes [38].

The first difference has several consequences. First, although one can solve Subgraph Matching via an MCS solver, the other way does not hold, i.e. one cannot use a Subgraph Matching solver for MCS detection, since Subgraph Matching has the stronger constraint of matching the entire q . Second, the stronger constraint of Subgraph Matching allows existing search algorithms to design pruning techniques as mentioned in the main text.

The second difference implies that the learning models designed for Subgraph Matching may not work well for MCS detection and vice versa. For example, N-BLS has a novel encoder layer with a matching module that has time complexity $\mathcal{O}(|V_q||\mathcal{A}_{u_t}|)$. However, if q becomes prohibitively large, e.g. as large as G containing millions of nodes, then the matching step would become a bottleneck and make the overall approach too slow to be useful in practice. Therefore, N-BLS cannot be used for MCS detection not only because fundamentally the search algorithm leverages the stronger constraint if Subgraph Matching, but also because the learning model would be inefficient and thus useless in practice. By the same reasoning, N-BLS is likely to be ineffective for graph isomorphism checking when both input graphs are of the same size and very large. This suggests the difficulty of designing a general neural network architecture that works efficiently and effectively for a series of related but different combinatorial optimization tasks. In theory, many such tasks are equivalent and can be converted to each other, but in practice, specialized models should be designed to render a truly useful learning-based approach.

A similar argument can be made for GLSEARCH [2] designed for MCS detection. GLSEARCH treats both input graphs symmetrically and does not leverage the fact that all the nodes and edges in q must be matched in G . The learning component GLSEARCH assumes both input graphs can be very large, and therefore instead of outputting a policy $P_\theta(a_t|s_t)$ for every action a_t at s_t , GLSEARCH performs the execution of each action to get its next state s_{t+1} , and compute the value associated with s_{t+1} for the $Q(s_t, a_t)$. This is named as “factoring out action” in [2], and requires sequentially going through all the actions to obtain the next states, for which GLSEARCH adopts a heuristic to reduce the amount of actions. To adapt GLSEARCH for Subgraph Matching, one has to use a heuristic to reduce the local candidate space, i.e. the action space, in order to be efficient enough to compare against existing solvers. In contrast, N-BLS efficiently computes one embedding per node for both q and G using the QC-SGMNN encoder layer, and computes $P_\theta(a_t|s_t)$ in the decoder by batching the node embeddings that are in the action space, i.e. $P_{\text{logit}}(a_t|s_t) = \text{MLP}(\text{CONCAT}(\mathbf{h}_{v_{a_t}}^T \mathbf{W}^{[1:F]} \mathbf{h}_{v_t}, \mathbf{h}_{s_t}))$ can be turned into a batch operation for all the node embeddings involved in the action space of s_t . The $v_\theta(s_t)$ is only needed during the training stage to enhance $P_\theta(a_t|s_t)$, and thus does not need to be predicted during inference.

In short, N-BLS cannot be used for large-input MCS detection due to the matching module performing matching between nodes in q and G , while GLSEARCH may be adapted for Subgraph Matching, it is likely to be ineffective due to the lack of policy network to efficiently compute a score for each pair of nodes leveraging the constraint of Subgraph Matching. We conduct experiments to adapt GLSEARCH for Subgraph Matching in Section E.3.

D Ablation Studies

We perform a series of ablation studies whose results are shown in Table 3. We find our key novelties indeed greatly contribute to N-BLS’s superior performance on Subgraph Matching, particularly the encoder-decoder design and bi-level search framework.

Table 3: Ablation study results on Subgraph Matching over DBLP Q_{128} . The ratio of the number of solved pairs over the 100 pairs is reported.

Model	DBLP Q_{128}
QUICKSI	0.07
GRAPHQL	0.02
CECI	0.18
DP-ISO	0.16
HYBRID	0.04
NMATCH	0.04
N-BLS	0.58
N-BLS-no-matching	0.25
N-BLS-GMN	0.51
N-BLS-no-MCTS	0.33
N-BLS-random	0.04

D.1 N-BLS without the Matching Module

We remove the matching module, and thus only perform the propagation module. The model is denoted as N-BLS-no-matching and achieves poor performance, which is expected, since we argue the matching module is the critical component in QC-SGMN to capture the state-dependent matching information.

D.2 N-BLS with GMN as the Matching Module

We notice the Graph Matching Network (GMN) [24] has a similar attention mechanism named as “cross-graph attention” that performs message passing between all the nodes in one graph and all the nodes in the other graph. However, GMN is designed for graph-graph similarity score approximation and thus does not consider the current state of matching s_t , and has a fixed quadratic time complexity. Figure 5 compares the two neural network architectures in details. Our QC-SGMN decouples the propagation and matching steps and outputs two sources of information separately, allowing the search to cache the state-independent node embeddings and dynamically select the computational paths during search. Our proposed QC-SGMN can be regarded as a state-dependent and Subgraph Matching suited graph matching neural network with efficiency in its design.

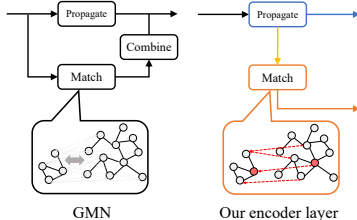


Figure 5: Comparison between GMN and QC-SGMN.

We replace the matching module with GMN, denoted as N-BLS-GMN. The result is worse than N-BLS but not by a large margin, suggesting the effectiveness of our matching module which is specialized for Subgraph Matching utilizing the state-dependent \tilde{M}_t mapping.

D.3 N-BLS without MCTS

We remove MCTS from the training stage, and instead compute the ground truth policy by simply observing the action that leads to the most reward during the training search process. We apply the same cross entropy loss function to train the policy network. The value network training procedure remains unchanged. The resulting trained model, N-BLS-no-MCTS, performs relatively poorly, as Monte Carlo Tree Search both balances the number of simulations performed on each search state sent to the replay buffer and estimates a more accurate ground truth policy.

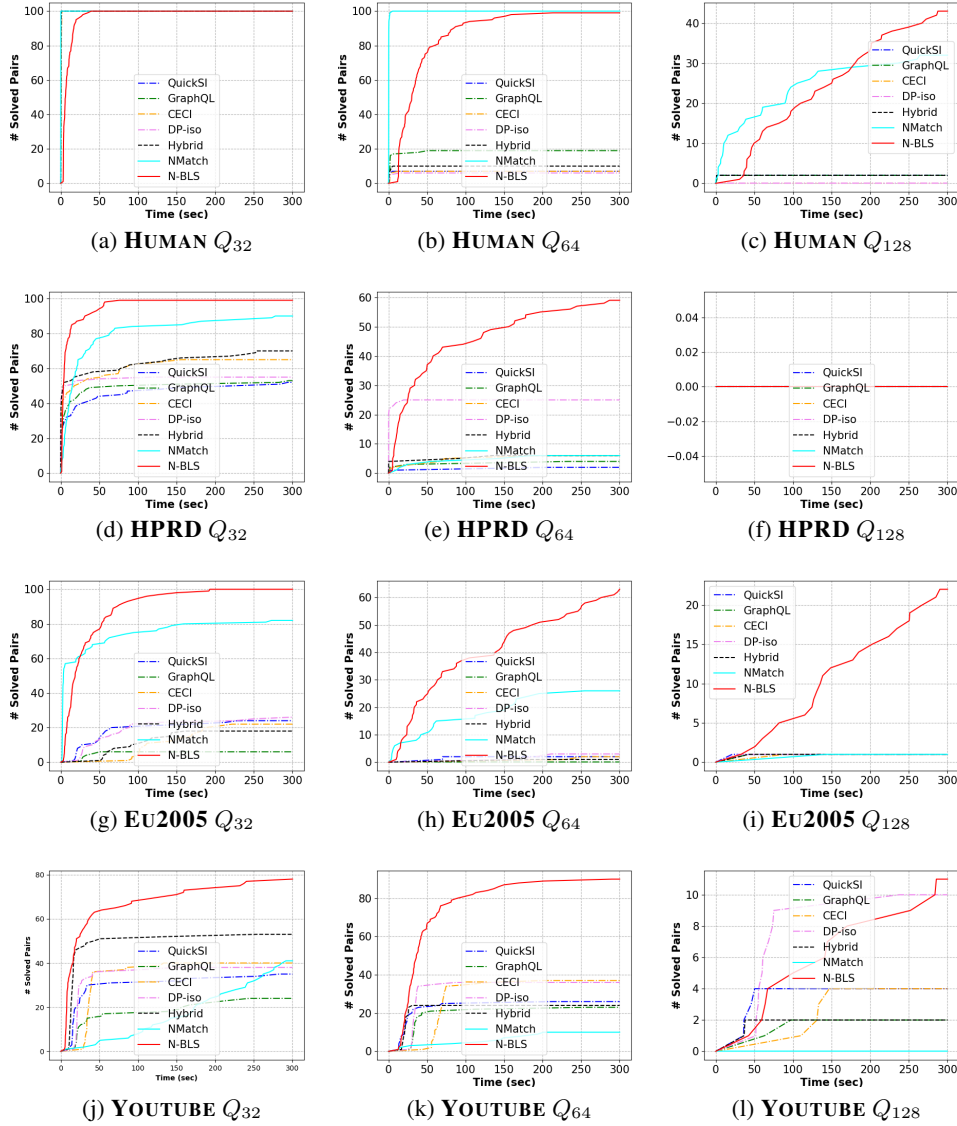


Figure 6: Comparison of the curves of the number of solved pairs versus time on HUMAN, HPRD, EU2005, and YOUTUBE. The plot for DBLP are shown in the main text.

D.4 N-BLS without training

To show that training indeed helps N-BLS, we run a random policy model, i.e. we let the search algorithm adopt a random policy. It is noteworthy that all the baseline solvers in C++ adopt a random policy for enumerating nodes in the candidate action space. Thus, N-BLS-random is equivalent to a Python version of the baseline solver using DP-ISO for filtering, GRAPHQL for query node ordering, and DP-ISO for local candidate computation. The fact that N-BLS-random can only match 4 pairs, the same as HYBRID and similar to GRAPHQL, suggests proper training of the policy network indeed is the key to the success of N-BLS.

E More Results with Analysis

E.1 Number of Solved Pairs Across Time

We provide figures on the number of solved pairs across time for all datasets in Figure 6, showing that N-BLS consistently solves more query graph pairs than baseline methods on most datasets. Figure 6 also shows N-BLS’s scalability with respect to query graph size, as baselines rapidly fail while N-BLS retains solid performance as query graphs get larger. Furthermore, the number of solutions found by baseline methods tend to flatten unlike N-BLS, which consistently solves more and more queries over time, suggesting that N-BLS will further outperform baselines if run for longer. We observe no clear correlation between the density of a query graph and the difficulty of solving the graph pair, i.e. the number of solutions found by the methods tested in our paper. We conjecture the difficulty is related to the distribution of the node degrees of a query graph, and leave the further investigation of predicting the difficulty of a graph pair without actually running a Subgraph Matching solver as future work.

E.2 Results on Running Time

We observe that the baseline solvers written in C++ have $O(1)$ time complexity for its random node selection policy for nodes in G , and thus tend to perform many more iterations than N-BLS written in Python during inference time. However, even with many more iterations performed by these baselines, they still fail to solve most pairs due to the too large action space incurred by the 128-node query graphs. Although 128 nodes do not seem to be very large, due to the combinatorial nature of Subgraph Matching, the search space is still intractable for these fast baselines. In contrast, our model written in Python is slower for each iteration but offers a much better overall result, suggesting good practicality and the promising research direction of designing learning-based strategy to enhance search algorithms.

We analyze the running time by showing the percentage of the major components in N-BLS. As shown in Figure 7, without caching the intra-graph node embeddings, the propagation module is the bottleneck, due to its $O(|E_q| + |E_G|)$ time complexity. It is noteworthy that we perform the propagation and matching modules sequentially to generate Figure 7 (a), i.e. for each QC-SGMNN, we first run the propagation module and then run the matching module. Although it is possible to further optimize the implementation by running two modules in parallel (to be specific, the propagation module of layer k and the matching module of layer $k - 1$ could be performed in parallel on two devices), we argue the bottleneck would still be the propagation module, for which the proposed caching technique would help. In comparison, by caching the state-independent $\mathbf{h}_{\text{intra}}^{(k)}$ node embeddings, the propagation module only takes 0.3% (corresponding to the almost invisible slice of red color) of the total running time budget (5 minutes).

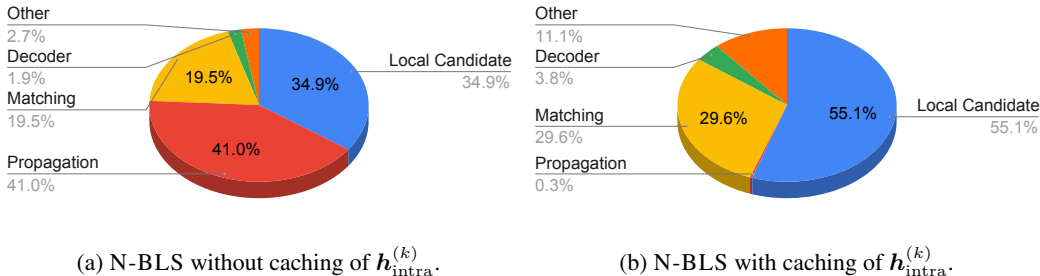


Figure 7: Running time breakdown by executing N-BLS (the inference stage) on one randomly sampled graph pair from EU2005 for 5 minutes and collecting the running time spent on each component. With caching, more iterations are performed due to each iteration being much faster.

We plot the change of global candidate space (CS) size and the local candidate space (LCS) size across time in Figure 8. Specifically, at each search iteration, a node u_t from the query graph is chosen by ϕ (line 7 of Algorithm 1 in the main text), and the local candidate space is computed for u_t (line 8 of Algorithm 1 in the main text). Therefore, we can record the number of candidates for u_t

in the global candidate space and in the local candidate space, and plot the change of CS and LCS sizes across search iterations. As shown in Figure 8, there is a large reduction of candidate nodes from CS to LCS, suggesting the importance of computing a smaller local candidate space based on the current matching and the selected u_t . Without any LCS computation technique, the action space would be the global CS, which may contain up to 100,000 nodes. Another important observation is that, the number of local candidate nodes varies dramatically across iterations. For example, in the initial iteration, since no nodes are matched, LCS is of the same size as CS, but as soon as one node pair is matched, the LCS computation can leverage the matched nodes by narrowing down the action space from all the nodes in CS to the first-order neighbors of the matched nodes. Existing LCS computation has several other techniques to reduce the candidate space size other than simply using the first-order neighbors of the matched subgraphs, and as a result, there can be less than 10 nodes in \mathcal{A}_{u_t} in some iterations. However, when the search backtracks to an earlier state, there can be more candidate nodes in LCS, resulting in the varying LCS sizes across search.

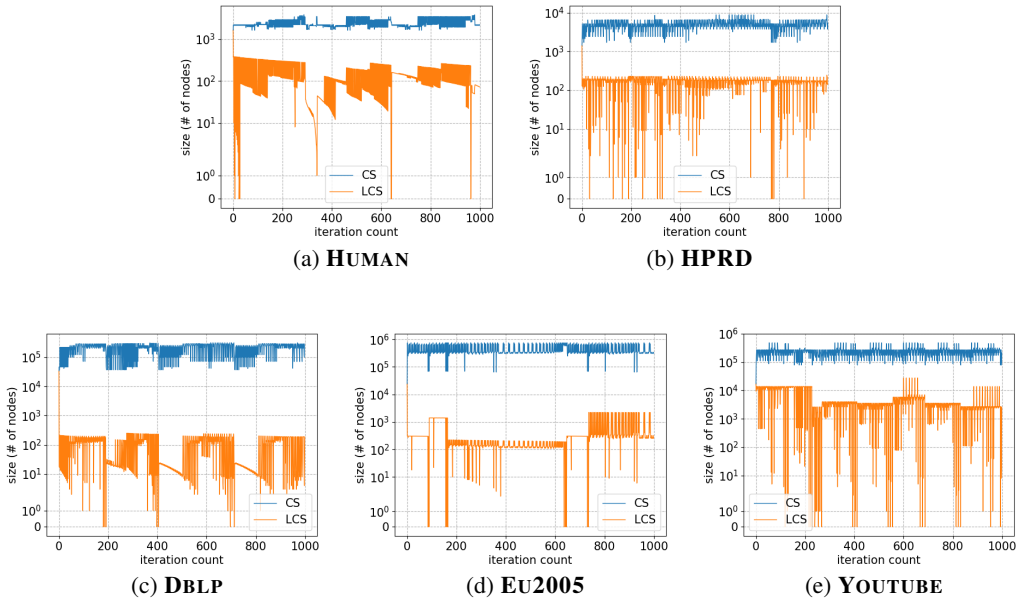


Figure 8: Demonstration of the sizes of global candidate space (CS) and local candidate space (LCS) across search iterations, by running N-BLS on a randomly sampled graph pair from each dataset, and collecting the size of CS and LCS at each search iteration. The y-axis is in the log scale. We stop recording the CS and LCS sizes after 1000 search iterations.

Since Figure 8 only shows the change of CS and LCS sizes across search for one graph pair, we show the statistics of CS and LCS sizes across 100 graph pairs in Table 4. Consistently with Figure 8, the LCS size is on average smaller than the CS size, suggesting the importance of LCS computation.

E.3 Results on Adapting GLSEARCH for Subgraph Matching

We report the performance of N-BLS and GLSEARCH on Subgraph Matching. As mentioned in Section C, Subgraph Matching contains a tighter set of constraints than MCS, causing GLSEARCH’s search framework to be less efficient and rely on a value-based model instead of a policy-based model. To measure the effects of both search framework and model design, we compare N-BLS to two models: (1) GLSEARCH, which uses the MCS search framework to conduct Subgraph Matching, and (2) GLSEARCH-ADAPTED, which uses the same value-based model architecture as GLSEARCH but adapted into N-BLS’s search framework. To ensure the efficiency of value-based models, which need to execute an action before computing the Q score, we adopt a simple sampling-based approach, where GLSEARCH-ADAPTED will always choose the best action out of up to 100 actions, regardless of the total action space size. We observe without such sampling, the model spends minutes executing a single action. Our results from Table 5 emphasizes the differences between Subgraph Matching and

Table 4: Statistics of the sizes of CS and LCS over 100 graph pairs for each dataset. “Avg”, “Min”, and “Max” denote average, minimum, and maximum, respectively.

Dataset Name	Avg	Min	Max
HUMAN Q_{128} (CS)	2217.65	395	4103
HUMAN Q_{128} (LCS)	55.65	0	1937
HPRD Q_{128} (CS)	4436.42	358	9031
HPRD Q_{128} (LCS)	25.03	0	1911
DBLP Q_{128} (CS)	170010.07	5370	317071
DBLP Q_{128} (LCS)	23.34	0	62127
EU2005 Q_{128} (CS)	612683.85	23327	861758
EU2005 Q_{128} (LCS)	337.65	0	623730
YOUTUBE Q_{128} (CS)	368211.15	13248	1134773
YOUTUBE Q_{128} (LCS)	55.79	0	118752

MCS by confirming the criticality of Subgraph Matching search constraints and N-BLS’s effective policy model design to Subgraph Matching performance.

Table 5: Results of directly applying and adapting GLSEARCH originally designed for MCS detection to Subgraph Matching.

Model	DBLP Q_{32}	DBLP Q_{64}	DBLP Q_{128}
N-BLS	1.00	0.97	0.58
GLSEARCH	0.0	0.0	0.0
GLSEARCH-ADAPTED	0.93	0.47	0.0

E.4 Reproducibility of Results

We run the trained N-BLS model for 3 times to study the expected variance in model performance, due to the fixed running time budget used in experiments, and the fact that N-BLS tends to solve more pairs towards the end of the 5-minute budget for each pair as shown in Figure 6. We find that N-BLS is able to reliably achieve good results on all datasets and outperform baseline methods. In contrast, baseline solvers in C++ tend to plateau and stop finding solutions for more pairs early in the 5-minute duration as seen in Figure 6.

Table 6: Reproducibility of the solved percentage results on the Q_{128} datasets.

Dataset	Mean	Stdev
HUMAN Q_{128}	0.53	0.09
HPRD Q_{128}	0.00	0.00
DBLP Q_{128}	0.62	0.03
EU2005 Q_{128}	0.23	0.03
YOUTUBE Q_{128}	0.11	0.01

E.5 Results on Labeled Graphs for Subgraph Matching

To test the generality of N-BLS, we compare it against baselines on a labeled dataset. By assigning labels, the filtering algorithm can further reduce the search space prior to the search process. Because of this, labeled datasets are generally easier than unlabeled datasets. The degree to which labels make Subgraph Matching easier is hard to determine. For instance, if all the target graph nodes in the same global candidate set share the same label, then the additional label constraint provides little guidance to search. On the other extreme, if each query graph node has a unique label that matches only one target graph node, then the search becomes trivial. For example, Knowledge Graph (KG) reasoning [31, 50] can also be viewed as matching a subgraph in a large KG, where a first-order logical query is represented as directed acyclic graph. However, since the KG can be incomplete with missing relations, exact Subgraph Matching may not be the most appropriate choice [31].

To be fair, we adopt the labeled EU2005 dataset provided by [38] for our experiment, where $|\Sigma| = 10$. Note, we do not retrain N-BLS on the labeled dataset, opting to use the same model trained on the unlabelled dataset. While node labels are not reflected in the initial features of the graph, they do shrink the size of the global and local candidate set, as only nodes with the same label can match each other.

Table 7: Results on labeled EU2005-labeled Q_{32} dataset. The ratio of the number of solved pairs over the 100 pairs is reported.

Model	EU2005-labeled Q_{32}
QUICKSI	0.35
GRAPHQL	0.72
CECI	0.70
DP-ISO	0.86
HYBRID	0.82
N-BLS	0.99

As seen in Table7, N-BLS outperforms baselines even on labeled graph instances, demonstrating its generality. This suggests the graph structure is very critical in Subgraph Matching search algorithms, even in the presence of other constraints such as node labels. We also tried such experiments on smaller datasets provided by [38], but found all methods were able to solve the graph pairs. As seen in Table 4, adding node labels to graphs with already small candidate sets could drastically reduce the search space, such that search space pruning on its own is enough to find a valid solution; however, as we have demonstrated thus far, there are many non-trivial cases where a smarter search policy, such as N-BLS, is required for Subgraph Matching. It is also possible to further improve N-BLS performance by training it on the labeled dataset, but we leave this as future work.

F Result Visualization

We show five instances of solved graph pairs by N-BLS in Figures 9, 10, 11, 12 and 13. We first plot (1) the query graph on its own, then plot (2) the query graph matched to the target graph, and finally plot (3) the target graph. In other words, the first and second plots correspond to the same query graph but their node positions/layouts are different. In the second plot we fix the positions of nodes in q to match the positions of their matched nodes in G , i.e. the nodes in the second and the third plots have the same relative node positions for visualizing the node-node mapping. The colors of nodes are for the purpose of visualizing the mapping. For clarity, we only show a subgraph of G instead of the entire G as it contains too many nodes and edges to show. Specifically, we include the matched q in G and grow the matched subgraph by including the first-order neighbors of the matched nodes.

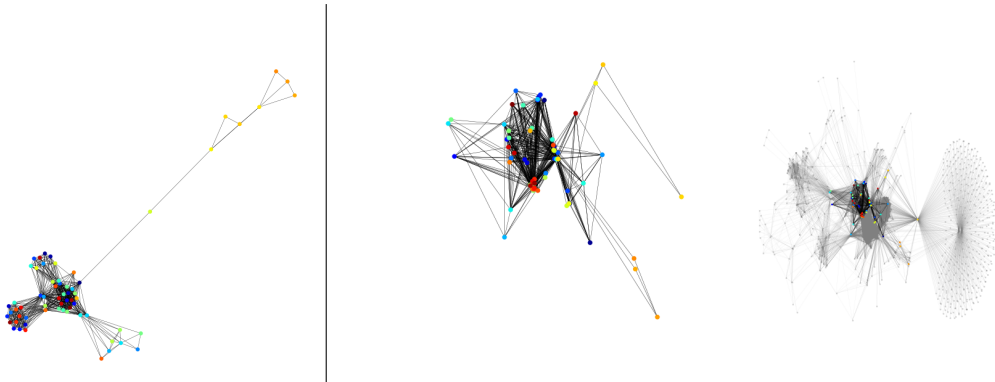


Figure 9: Visualization of a solved pair on HUMAN Q_{64} .

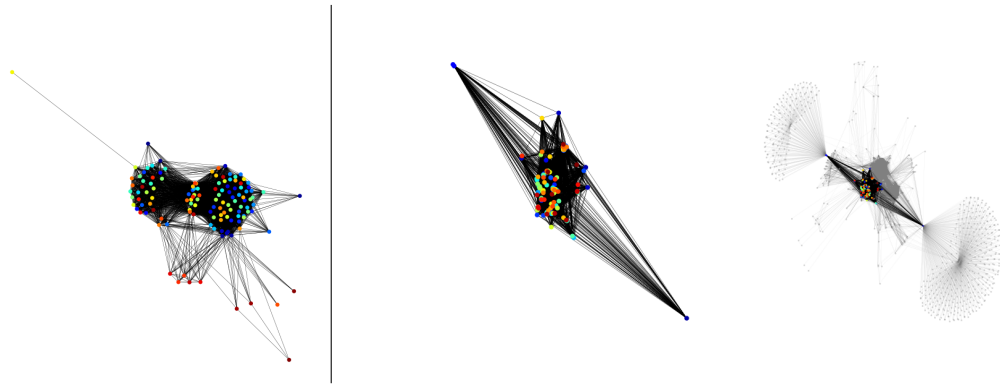


Figure 10: Visualization of a solved pair on HUMAN Q_{128} .

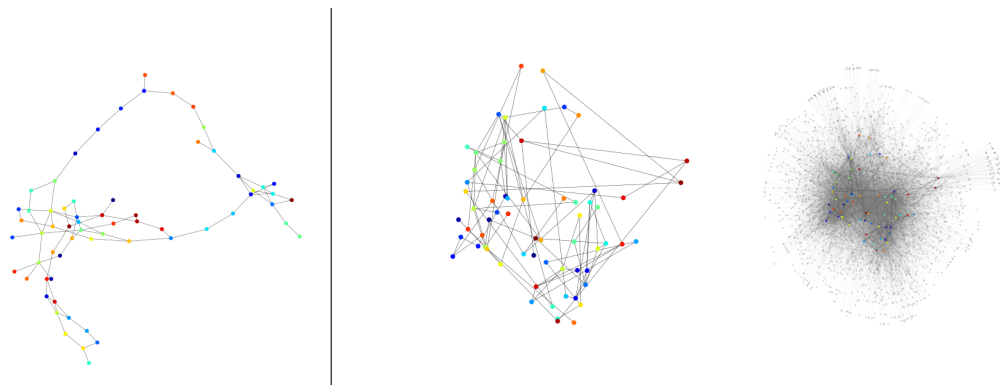


Figure 11: Visualization of a solved pair on HPRD Q_{64} .

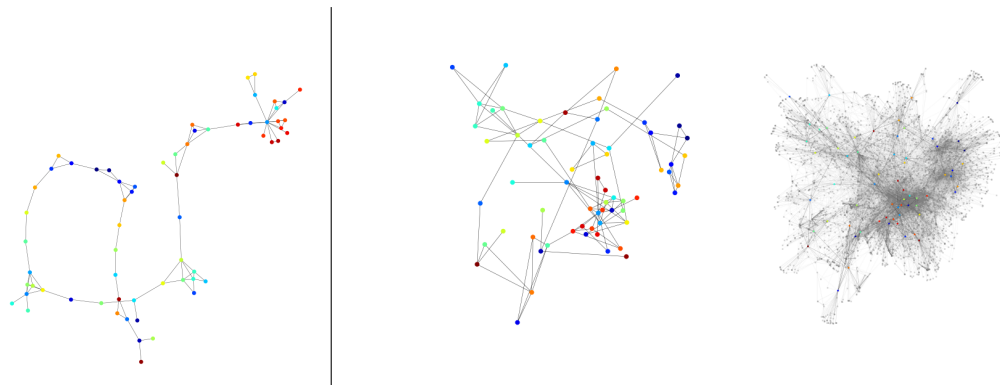


Figure 12: Visualization of a solved pair on DBLP Q_{64} .

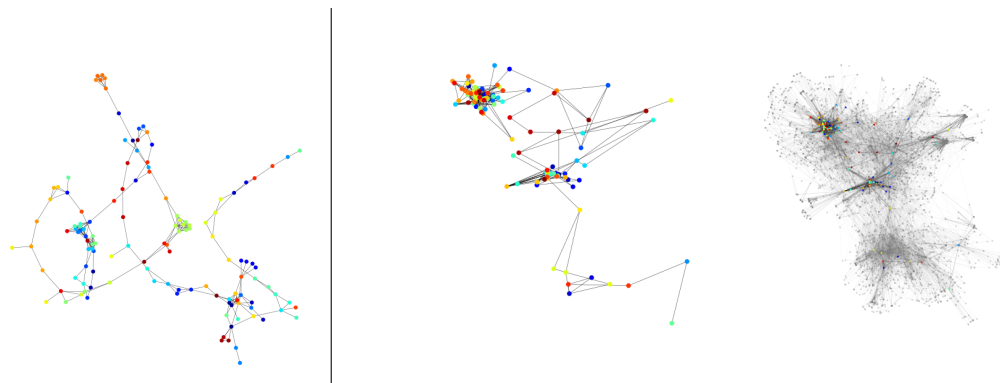


Figure 13: Visualization of a solved pair on DBLP Q_{128} .

References

- [1] Jimmy Lei Ba, Jamie Ryan Kiros, and Geoffrey E Hinton. Layer normalization. *arXiv preprint arXiv:1607.06450*, 2016.
- [2] Yunsheng Bai, Derek Xu, Yizhou Sun, and Wei Wang. Gsearch: Maximum common subgraph detection via learning to search. In *ICML*, pages 588–598. PMLR, 2021.
- [3] Bibek Bhattacharai, Hang Liu, and H Howie Huang. Ceci: Compact embedding cluster index for scalable subgraph matching. In *Proceedings of the 2019 International Conference on Management of Data*, pages 1447–1462, 2019.
- [4] Vincenzo Bonnici, Rosalba Giugno, Alfredo Pulvirenti, Dennis Shasha, and Alfredo Ferro. A subgraph isomorphism algorithm and its application to biochemical data. *BMC bioinformatics*, 14(7):1–13, 2013.
- [5] Shaked Brody, Uri Alon, and Eran Yahav. How attentive are graph attention networks? *ICLR*, 2022.
- [6] Cameron B Browne, Edward Powley, Daniel Whitehouse, Simon M Lucas, Peter I Cowling, Philipp Rohlfshagen, Stephen Tavener, Diego Perez, Spyridon Samothrakis, and Simon Colton. A survey of monte carlo tree search methods. *IEEE Transactions on Computational Intelligence and AI in games*, 4(1):1–43, 2012.
- [7] Chen Cai and Yusu Wang. A simple yet effective baseline for non-attributed graph classification. *arXiv preprint arXiv:1811.03508*, 2018.
- [8] Zhengdao Chen, Lei Chen, Soledad Villar, and Joan Bruna. Can graph neural networks count substructures? *NeurIPS*, 33:10383–10395, 2020.
- [9] Anthony DiGiovanni and Ethan C Zell. Survey of self-play in reinforcement learning. *arXiv preprint arXiv:2107.02850*, 2021.
- [10] Myoungji Han, Hyunjoon Kim, Geonmo Gu, Kunsu Park, and Wook-Shin Han. Efficient subgraph matching: Harmonizing dynamic programming, adaptive matching order, and failing set together. In *Proceedings of the 2019 International Conference on Management of Data*, pages 1429–1446, 2019.
- [11] Wook-Shin Han, Jinsoo Lee, and Jeong-Hoon Lee. Turboiso: towards ultrafast and robust subgraph isomorphism search in large graph databases. In *Proceedings of the 2013 ACM SIGMOD International Conference on Management of Data*, pages 337–348, 2013.
- [12] Huahai He and Ambuj K Singh. Graphs-at-a-time: query language and access methods for graph databases. In *Proceedings of the 2008 ACM SIGMOD international conference on Management of data*, pages 405–418, 2008.
- [13] Hui Jiang, Yuxin Deng, and Ming Xu. Quantum circuit transformation based on subgraph isomorphism and tabu search. *arXiv e-prints*, pages arXiv–2104, 2021.
- [14] Chathura Kankanamge, Siddhartha Sahu, Amine Mhedbhi, Jeremy Chen, and Semih Salihoglu. Graphflow: An active graph database. In *Proceedings of the 2017 ACM International Conference on Management of Data*, pages 1695–1698, 2017.
- [15] Hyunjoon Kim, Yunyoung Choi, Kunsu Park, Xuemin Lin, Seok-Hee Hong, and Wook-Shin Han. Versatile equivalences: Speeding up subgraph query processing and subgraph matching. In *Proceedings of the 2021 International Conference on Management of Data*, pages 925–937, 2021.
- [16] Jinha Kim, Hyungyu Shin, Wook-Shin Han, Sungpack Hong, and Hassan Chafi. Taming subgraph isomorphism for rdf query processing. *arXiv preprint arXiv:1506.01973*, 2015.
- [17] Diederik P Kingma and Jimmy Ba. Adam: A method for stochastic optimization. *ICLR*, 2015.
- [18] Thomas N Kipf and Max Welling. Semi-supervised classification with graph convolutional networks. *ICLR*, 2016.

- [19] Levente Kocsis and Csaba Szepesvári. Bandit based monte-carlo planning. In *European conference on machine learning*, pages 282–293. Springer, 2006.
- [20] Longbin Lai, Lu Qin, Xuemin Lin, and Lijun Chang. Scalable subgraph enumeration in mapreduce. *Proceedings of the VLDB Endowment*, 8(10):974–985, 2015.
- [21] Longbin Lai, Lu Qin, Xuemin Lin, Ying Zhang, Lijun Chang, and Shiyu Yang. Scalable distributed subgraph enumeration. *Proceedings of the VLDB Endowment*, 10(3):217–228, 2016.
- [22] Longbin Lai, Zhu Qing, Zhengyi Yang, Xin Jin, Zhengmin Lai, Ran Wang, Kongzhang Hao, Xuemin Lin, Lu Qin, Wenjie Zhang, et al. Distributed subgraph matching on timely dataflow. *Proceedings of the VLDB Endowment*, 12(10):1099–1112, 2019.
- [23] Jinsoo Lee, Wook-Shin Han, Romans Kasperovics, and Jeong-Hoon Lee. An in-depth comparison of subgraph isomorphism algorithms in graph databases. *Proceedings of the VLDB Endowment*, 6(2):133–144, 2012.
- [24] Yujia Li, Chenjie Gu, Thomas Dullien, Oriol Vinyals, and Pushmeet Kohli. Graph matching networks for learning the similarity of graph structured objects. *ICML*, 2019.
- [25] Xin Liu, Haojie Pan, Mutian He, Yangqiu Song, Xin Jiang, and Lifeng Shang. Neural subgraph isomorphism counting. In *Proceedings of the 26th ACM SIGKDD International Conference on Knowledge Discovery & Data Mining*, pages 1959–1969, 2020.
- [26] Zhaoyu Lou, Jiaxuan You, Chengtao Wen, Arquimedes Canedo, Jure Leskovec, et al. Neural subgraph matching. *arXiv preprint arXiv:2007.03092*, 2020.
- [27] Tinghuai Ma, Siyang Yu, Jie Cao, Yuan Tian, Abdullah Al-Dhelaan, and Mznah Al-Rodhaan. A comparative study of subgraph matching isomorphic methods in social networks. *IEEE Access*, 6:66621–66631, 2018.
- [28] Ciaran McCreesh, Patrick Prosser, Christine Solnon, and James Trimble. When subgraph isomorphism is really hard, and why this matters for graph databases. *Journal of Artificial Intelligence Research*, 61:723–759, 2018.
- [29] Christopher Morris, Gaurav Rattan, and Petra Mutzel. Weisfeiler and leman go sparse: Towards scalable higher-order graph embeddings. *NeurIPS*, 33:21824–21840, 2020.
- [30] Diego Perez-Liebana, Jialin Liu, Ahmed Khalifa, Raluca D Gaina, Julian Togelius, and Simon M Lucas. General video game ai: A multitrack framework for evaluating agents, games, and content generation algorithms. *IEEE Transactions on Games*, 11(3):195–214, 2019.
- [31] Hongyu Ren, Weihua Hu, and Jure Leskovec. Query2box: Reasoning over knowledge graphs in vector space using box embeddings. *ICLR*, 2020.
- [32] Oliver Richter and Roger Wattenhofer. Normalized attention without probability cage. *arXiv preprint arXiv:2005.09561*, 2020.
- [33] Julian Schrittwieser, Ioannis Antonoglou, Thomas Hubert, Karen Simonyan, Laurent Sifre, Simon Schmitt, Arthur Guez, Edward Lockhart, Demis Hassabis, Thore Graepel, et al. Mastering atari, go, chess and shogi by planning with a learned model. *Nature*, 588(7839):604–609, 2020.
- [34] Haichuan Shang, Ying Zhang, Xuemin Lin, and Jeffrey Xu Yu. Taming verification hardness: an efficient algorithm for testing subgraph isomorphism. *Proceedings of the VLDB Endowment*, 1(1):364–375, 2008.
- [35] David Silver, Thomas Hubert, Julian Schrittwieser, Ioannis Antonoglou, Matthew Lai, Arthur Guez, Marc Lanctot, Laurent Sifre, Dharrshan Kumaran, Thore Graepel, et al. A general reinforcement learning algorithm that masters chess, shogi, and go through self-play. *Science*, 362(6419):1140–1144, 2018.
- [36] David Silver, Julian Schrittwieser, Karen Simonyan, Ioannis Antonoglou, Aja Huang, Arthur Guez, Thomas Hubert, Lucas Baker, Matthew Lai, Adrian Bolton, et al. Mastering the game of go without human knowledge. *nature*, 550(7676):354–359, 2017.

- [37] Samuel Sokota, Caleb Y Ho, Zaheen Ahmad, and J Zico Kolter. Monte carlo tree search with iteratively refining state abstractions. *NeurIPS*, 34:18698–18709, 2021.
- [38] Shixuan Sun and Qiong Luo. In-memory subgraph matching: An in-depth study. In *Proceedings of the 2020 ACM SIGMOD International Conference on Management of Data*, pages 1083–1098, 2020.
- [39] Shixuan Sun, Xibo Sun, Yulin Che, Qiong Luo, and Bingsheng He. Rapidmatch: a holistic approach to subgraph query processing. *Proceedings of the VLDB Endowment*, 14(2):176–188, 2020.
- [40] Ashish Vaswani, Noam Shazeer, Niki Parmar, Jakob Uszkoreit, Llion Jones, Aidan N Gomez, Lukasz Kaiser, and Illia Polosukhin. Attention is all you need. *Advances in neural information processing systems*, 30, 2017.
- [41] Todd L Veldhuizen. Leapfrog triejoin: A simple, worst-case optimal join algorithm. *arXiv preprint arXiv:1210.0481*, 2012.
- [42] Petar Velickovic, Guillem Cucurull, Arantxa Casanova, Adriana Romero, Pietro Lio, and Yoshua Bengio. Graph attention networks. *ICLR*, 2018.
- [43] Hanchen Wang, Ying Zhang, Lu Qin, Wei Wang, Wenjie Zhang, and Xuemin Lin. Reinforcement learning based query vertex ordering model for subgraph matching. *arXiv preprint arXiv:2201.11251*, 2022.
- [44] Runzhong Wang, Zhigang Hua, Gan Liu, Jiayi Zhang, Junchi Yan, Feng Qi, Shuang Yang, Jun Zhou, and Xiaokang Yang. A bi-level framework for learning to solve combinatorial optimization on graphs. *NeurIPS*, 34, 2021.
- [45] Asiri Wijesinghe and Qing Wang. A new perspective on "how graph neural networks go beyond weisfeiler-lehman?". In *ICLR*, 2022.
- [46] Zhihao Xing and Shikui Tu. A graph neural network assisted monte carlo tree search approach to traveling salesman problem. *IEEE Access*, 8:108418–108428, 2020.
- [47] Keyulu Xu, Chengtao Li, Yonglong Tian, Tomohiro Sonobe, Ken-ichi Kawarabayashi, and Stefanie Jegelka. Representation learning on graphs with jumping knowledge networks. *ICML*, 2018.
- [48] Jiaxuan You, Zhitao Ying, and Jure Leskovec. Design space for graph neural networks. *NeurIPS*, 33:17009–17021, 2020.
- [49] Shijie Zhang, Shirong Li, and Jiong Yang. Gaddi: distance index based subgraph matching in biological networks. In *Proceedings of the 12th International Conference on Extending Database Technology: Advances in Database Technology*, pages 192–203, 2009.
- [50] Zhanqiu Zhang, Jie Wang, Jiajun Chen, Shuiwang Ji, and Feng Wu. Cone: Cone embeddings for multi-hop reasoning over knowledge graphs. *NeurIPS*, 34, 2021.